

Measurement of $B \rightarrow K^* \gamma$ Branching Fractions and Charge Asymmetries

B. Aubert,¹ D. Boutigny,¹ J.-M. Gaillard,¹ A. Hicheur,¹ Y. Karyotakis,¹ J.P. Lees,¹ P. Robbe,¹ V. Tisserand,¹ A. Palano,² G.P. Chen,³ J.C. Chen,³ N.D. Qi,³ G. Rong,³ P. Wang,³ Y.S. Zhu,³ G. Eigen,⁴ P.L. Reinertsen,⁴ B. Stugu,⁴ B. Abbott,⁵ G.S. Abrams,⁵ A.W. Borgland,⁵ A.B. Breon,⁵ D.N. Brown,⁵ J. Button-Shafer,⁵ R.N. Cahn,⁵ A.R. Clark,⁵ M.S. Gill,⁵ A.V. Gritsan,⁵ Y. Groyzman,⁵ R.G. Jacobsen,⁵ R.W. Kadel,⁵ J. Kadyk,⁵ L.T. Kerth,⁵ S. Kluth,⁵ Yu. G. Kolomensky,⁵ J.F. Kral,⁵ C. LeClerc,⁵ M.E. Levi,⁵ T. Liu,⁵ G. Lynch,⁵ A.B. Meyer,⁵ M. Momayezi,⁵ P.J. Oddone,⁵ A. Perazzo,⁵ M. Pripstein,⁵ N.A. Roe,⁵ A. Romosan,⁵ M.T. Ronan,⁵ V.G. Shelkov,⁵ A.V. Telnov,⁵ W.A. Wenzel,⁵ M.S. Zisman,⁵ P.G. Bright-Thomas,⁶ T.J. Harrison,⁶ C.M. Hawkes,⁶ D.J. Knowles,⁶ S.W. O'Neale,⁶ R.C. Penny,⁶ A.T. Watson,⁶ N.K. Watson,⁶ T. Deppermann,⁷ K. Goetzen,⁷ H. Koch,⁷ J. Krug,⁷ M. Kunze,⁷ B. Lewandowski,⁷ K. Peters,⁷ H. Schmuecker,⁷ M. Steinke,⁷ J.C. Andress,⁸ N.R. Barlow,⁸ W. Bhimji,⁸ N. Chevalier,⁸ P.J. Clark,⁸ W.N. Cottingham,⁸ N. De Groot,⁸ N. Dyce,⁸ B. Foster,⁸ J.D. McFall,⁸ D. Wallom,⁸ F.F. Wilson,⁸ K. Abe,⁹ C. Hearty,⁹ T.S. Mattison,⁹ J.A. McKenna,⁹ D. Thiessen,⁹ S. Jolly,¹⁰ A.K. McKemey,¹⁰ J. Tinslay,¹⁰ V.E. Blinov,¹¹ A.D. Bukin,¹¹ D.A. Bukin,¹¹ A.R. Buzykaev,¹¹ V.B. Golubev,¹¹ V.N. Ivanchenko,¹¹ A.A. Korol,¹¹ E.A. Kravchenko,¹¹ A.P. Onuchin,¹¹ A.A. Salnikov,¹¹ S.I. Serednyakov,¹¹ Yu.I. Skovpen,¹¹ V.I. Telnov,¹¹ A.N. Yushkov,¹¹ D. Best,¹² A.J. Lankford,¹² M. Mandelkern,¹² S. McMahon,¹² D.P. Stoker,¹² A. Ahsan,¹³ K. Arisaka,¹³ C. Buchanan,¹³ S. Chun,¹³ J.G. Branson,¹⁴ D.B. MacFarlane,¹⁴ S. Prell,¹⁴ Sh. Rahatlou,¹⁴ G. Raven,¹⁴ V. Sharma,¹⁴ C. Campagnari,¹⁵ B. Dahmes,¹⁵ P.A. Hart,¹⁵ N. Kuznetsova,¹⁵ S.L. Levy,¹⁵ O. Long,¹⁵ A. Lu,¹⁵ J.D. Richman,¹⁵ W. Verkerke,¹⁵ M. Witherell,¹⁵ S. Yellin,¹⁵ J. Beringer,¹⁶ D.E. Dorfan,¹⁶ A.M. Eisner,¹⁶ A. Frey,¹⁶ A.A. Grillo,¹⁶ M. Grothe,¹⁶ C.A. Heusch,¹⁶ R.P. Johnson,¹⁶ W. Kroeger,¹⁶ W.S. Lockman,¹⁶ T. Pulliam,¹⁶ H. Sadrozinski,¹⁶ T. Schalk,¹⁶ R.E. Schmitz,¹⁶ B.A. Schumm,¹⁶ A. Seiden,¹⁶ M. Turri,¹⁶ W. Walkowiak,¹⁶ D.C. Williams,¹⁶ M.G. Wilson,¹⁶ E. Chen,¹⁷ G.P. Dubois-Felsmann,¹⁷ A. Dvoretzki,¹⁷ D.G. Hitlin,¹⁷ S. Metzler,¹⁷ J. Oyang,¹⁷ F.C. Porter,¹⁷ A. Ryd,¹⁷ A. Samuel,¹⁷ M. Weaver,¹⁷ S. Yang,¹⁷ R.Y. Zhu,¹⁷ S. Devmal,¹⁸ T.L. Geld,¹⁸ S. Jayatilleke,¹⁸ G. Mancinelli,¹⁸ B.T. Meadows,¹⁸ M.D. Sokoloff,¹⁸ T. Barillari,¹⁹ P. Bloom,¹⁹ M.O. Dima,¹⁹ S. Fahey,¹⁹ W.T. Ford,¹⁹ D.R. Johnson,¹⁹ U. Nauenberg,¹⁹ A. Olivas,¹⁹ H. Park,¹⁹ P. Rankin,¹⁹ J. Roy,¹⁹ S. Sen,¹⁹ J.G. Smith,¹⁹ W.C. van Hoek,¹⁹ D.L. Wagner,¹⁹ J. Blouw,²⁰ J.L. Harton,²⁰ M. Krishnamurthy,²⁰ A. Soffer,²⁰ W.H. Toki,²⁰ R.J. Wilson,²⁰ J. Zhang,²⁰ T. Brandt,²¹ J. Brose,²¹ T. Colberg,²¹ G. Dahlinger,²¹ M. Dickopp,²¹ R.S. Dubitzky,²¹ A. Hauke,²¹ E. Maly,²¹ R. Müller-Pfefferkorn,²¹ S. Otto,²¹ K.R. Schubert,²¹ R. Schwierz,²¹ B. Spaan,²¹ L. Wilden,²¹ L. Behr,²² D. Bernard,²² G.R. Bonneaud,²² F. Brochard,²² J. Cohen-Tanugi,²² S. Ferrag,²² E. Rousot,²² S. T'Jampens,²² Ch. Thiebaux,²² G. Vasileiadis,²² M. Verderi,²² A. Anjomshoaa,²³ R. Bernet,²³ A. Khan,²³ D. Lavin,²³ F. Muheim,²³ S. Playfer,²³ J.E. Swain,²³ M. Falbo,²⁴ C. Borean,²⁵ C. Bozzi,²⁵ S. Dittongo,²⁵ M. Folegani,²⁵ L. Piemontese,²⁵ E. Treadwell,²⁶ F. Anulli,^{27,*} R. Baldini-Feroli,²⁷ A. Calcaterra,²⁷ R. de Sangro,²⁷ D. Falciari,²⁷ G. Finocchiaro,²⁷ P. Patteri,²⁷ I.M. Peruzzi,^{27,*} M. Piccolo,²⁷ Y. Xie,²⁷ A. Zallo,²⁷ S. Bagnasco,²⁸ A. Buzzo,²⁸ R. Contri,²⁸ G. Crosetti,²⁸ P. Fabbriatore,²⁸ S. Farinon,²⁸ M. Lo Vetere,²⁸ M. Macri,²⁸ M.R. Monge,²⁸ R. Musenich,²⁸ M. Pallavicini,²⁸ R. Parodi,²⁸ S. Passaggio,²⁸ F.C. Pastore,²⁸ C. Patrignani,²⁸ M.G. Pia,²⁸ C. Priano,²⁸ E. Robutti,²⁸ A. Santroni,²⁸ M. Morii,²⁹ R. Bartoldus,³⁰ T. Dignan,³⁰ R. Hamilton,³⁰ U. Mallik,³⁰ J. Cochran,³¹ H.B. Crawley,³¹ P.-A. Fischer,³¹ J. Lamsa,³¹ W.T. Meyer,³¹ E.I. Rosenberg,³¹ M. Benkebil,³² G. Grosdidier,³² C. Hast,³² A. Höcker,³² H.M. Lacker,³² S. Laplace,³² V. Lepeltier,³² A.M. Lutz,³² S. Plaszczynski,³² M.H. Schune,³² S. Trincaz-Duvoid,³² A. Valassi,³² G. Wormser,³² R.M. Bionta,³³ V. Brigljević,³³ D.J. Lange,³³ M. Mugge,³³ X. Shi,³³ K. van Bibber,³³ T.J. Wenaus,³³ D.M. Wright,³³ C.R. Wuest,³³ M. Carroll,³⁴ J.R. Fry,³⁴ E. Gabathuler,³⁴ R. Gamet,³⁴ M. George,³⁴ M. Kay,³⁴ D.J. Payne,³⁴ R.J. Sloane,³⁴ C. Touramanis,³⁴ M.L. Aspinwall,³⁵ D.A. Bowerman,³⁵ P.D. Dauncey,³⁵ U. Egede,³⁵ I. Eschrich,³⁵ N.J.W. Gunawardane,³⁵ J.A. Nash,³⁵ P. Sanders,³⁵ D. Smith,³⁵ D.E. Azzopardi,³⁶ J.J. Back,³⁶ P. Dixon,³⁶ P.F. Harrison,³⁶ R.J.L. Potter,³⁶ H.W. Shorthouse,³⁶ P. Strother,³⁶ P.B. Vidal,³⁶ M.I. Williams,³⁶ G. Cowan,³⁷ S. George,³⁷ M.G. Green,³⁷ A. Kurup,³⁷ C.E. Marker,³⁷ P. McGrath,³⁷ T.R. McMahon,³⁷ S. Ricciardi,³⁷ F. Salvatore,³⁷ I. Scott,³⁷ G. Vaitsas,³⁷ D. Brown,³⁸ C.L. Davis,³⁸ J. Allison,³⁹ R.J. Barlow,³⁹ J.T. Boyd,³⁹ A.C. Forti,³⁹ J. Fullwood,³⁹ F. Jackson,³⁹ G.D. Lafferty,³⁹ N. Savvas,³⁹ E.T. Simopoulos,³⁹ J.H. Weatherall,³⁹ A. Farbin,⁴⁰ A. Jawahery,⁴⁰ V. Lillard,⁴⁰ J. Olsen,⁴⁰ D.A. Roberts,⁴⁰ J.R. Schieck,⁴⁰ G. Blaylock,⁴¹ C. Dallapiccola,⁴¹ K.T. Flood,⁴¹ S.S. Hertzbach,⁴¹ R. Kofler,⁴¹ T.B. Moore,⁴¹ H. Staengle,⁴¹ S. Willocq,⁴¹ B. Brau,⁴² R. Cowan,⁴² G. Sciolla,⁴² F. Taylor,⁴² R.K. Yamamoto,⁴² M. Milek,⁴³ P.M. Patel,⁴³ J. Trischuk,⁴³ F. Lanni,⁴⁴ F. Palombo,⁴⁴ J.M. Bauer,⁴⁵ M. Booke,⁴⁵ L. Cremaldi,⁴⁵ V. Eschenburg,⁴⁵ R. Kroeger,⁴⁵ J. Reidy,⁴⁵ D.A. Sanders,⁴⁵ D.J. Summers,⁴⁵ J.P. Martin,⁴⁶ J.Y. Nief,⁴⁶ R. Seitz,⁴⁶ P. Taras,⁴⁶ V. Zacek,⁴⁶

H. Nicholson,⁴⁷ C. S. Sutton,⁴⁷ C. Cartaro,⁴⁸ N. Cavallo,^{48,†} G. De Nardo,⁴⁸ F. Fabozzi,⁴⁸ C. Gatto,⁴⁸ L. Lista,⁴⁸ P. Paolucci,⁴⁸ D. Piccolo,⁴⁸ C. Sciacca,⁴⁸ J. M. LoSecco,⁴⁹ J. R. G. Alsmiller,⁵⁰ T. A. Gabriel,⁵⁰ T. Handler,⁵⁰ J. Brau,⁵¹ R. Frey,⁵¹ M. Iwasaki,⁵¹ N. B. Sinev,⁵¹ D. Strom,⁵¹ F. Colecchia,⁵² F. Dal Corso,⁵² A. Dorigo,⁵² F. Galeazzi,⁵² M. Margoni,⁵² G. Michelon,⁵² M. Morandin,⁵² M. Posocco,⁵² M. Rotondo,⁵² F. Simonetto,⁵² R. Stroili,⁵² E. Torassa,⁵² C. Voci,⁵² M. Benayoun,⁵³ H. Briand,⁵³ J. Chauveau,⁵³ P. David,⁵³ Ch. de la Vaissière,⁵³ L. Del Buono,⁵³ O. Hamon,⁵³ F. Le Diberder,⁵³ Ph. Leruste,⁵³ J. Lory,⁵³ L. Roos,⁵³ J. Stark,⁵³ S. Versillé,⁵³ P. F. Manfredi,⁵⁴ V. Re,⁵⁴ V. Speziali,⁵⁴ E. D. Frank,⁵⁵ L. Gladney,⁵⁵ Q. H. Guo,⁵⁵ J. H. Panetta,⁵⁵ C. Angelini,⁵⁶ G. Batignani,⁵⁶ S. Bettarini,⁵⁶ M. Bondioli,⁵⁶ M. Carpinelli,⁵⁶ F. Forti,⁵⁶ M. A. Giorgi,⁵⁶ A. Lusiani,⁵⁶ F. Martinez-Vidal,⁵⁶ M. Morganti,⁵⁶ N. Neri,⁵⁶ E. Paoloni,⁵⁶ M. Rama,⁵⁶ G. Rizzo,⁵⁶ F. Sandrelli,⁵⁶ G. Simi,⁵⁶ G. Triggiani,⁵⁶ J. Walsh,⁵⁶ M. Haire,⁵⁷ D. Judd,⁵⁷ K. Paick,⁵⁷ L. Turnbull,⁵⁷ D. E. Wagoner,⁵⁷ J. Albert,⁵⁸ C. Bula,⁵⁸ P. Elmer,⁵⁸ C. Lu,⁵⁸ K. T. McDonald,⁵⁸ V. Miftakov,⁵⁸ S. F. Schaffner,⁵⁸ A. J. S. Smith,⁵⁸ A. Tumanov,⁵⁸ E. W. Varnes,⁵⁸ G. Cavoto,⁵⁹ D. del Re,⁵⁹ R. Faccini,^{14,59} F. Ferrarotto,⁵⁹ F. Ferroni,⁵⁹ K. Fratini,⁵⁹ E. Lamanna,⁵⁹ E. Leonardi,⁵⁹ M. A. Mazzoni,⁵⁹ S. Morganti,⁵⁹ G. Piredda,⁵⁹ F. Safai Tehrani,⁵⁹ M. Serra,⁵⁹ C. Voena,⁵⁹ S. Christ,⁶⁰ R. Waldi,⁶⁰ T. Adye,⁶¹ B. Franek,⁶¹ N. I. Geddes,⁶¹ G. P. Gopal,⁶¹ S. M. Xella,⁶¹ R. Aleksan,⁶² G. De Domenico,⁶² S. Emery,⁶² A. Gaidot,⁶² S. F. Ganzhur,⁶² P.-F. Giraud,⁶² G. Hamel Monchenault,⁶² W. Kozanecki,⁶² M. Langer,⁶² G. W. London,⁶² B. Mayer,⁶² B. Serfass,⁶² G. Vasseur,⁶² Ch. Yèche,⁶² M. Zito,⁶² N. Coptý,⁶³ M. V. Purohit,⁶³ H. Singh,⁶³ F. X. Yumiceva,⁶³ I. Adam,⁶⁴ P. L. Anthony,⁶⁴ D. Aston,⁶⁴ K. Baird,⁶⁴ J. P. Berger,⁶⁴ E. Bloom,⁶⁴ A. M. Boyarski,⁶⁴ F. Bulos,⁶⁴ G. Calderini,⁶⁴ R. Claus,⁶⁴ M. R. Convery,⁶⁴ D. P. Coupal,⁶⁴ D. H. Coward,⁶⁴ J. Dorfan,⁶⁴ M. Doser,⁶⁴ W. Dunwoodie,⁶⁴ R. C. Field,⁶⁴ T. Glanzman,⁶⁴ G. L. Godfrey,⁶⁴ S. J. Gowdy,⁶⁴ P. Grosso,⁶⁴ T. Himel,⁶⁴ T. Hryn'ova,⁶⁴ M. E. Huffer,⁶⁴ W. R. Innes,⁶⁴ C. P. Jessop,⁶⁴ M. H. Kelsey,⁶⁴ P. Kim,⁶⁴ M. L. Kocian,⁶⁴ U. Langenegger,⁶⁴ D. W. G. S. Leith,⁶⁴ S. Luitz,⁶⁴ V. Luth,⁶⁴ H. L. Lynch,⁶⁴ H. Marsiske,⁶⁴ S. Menke,⁶⁴ R. Messner,⁶⁴ K. C. Moffeit,⁶⁴ R. Mount,⁶⁴ D. R. Muller,⁶⁴ C. P. O'Grady,⁶⁴ M. Perl,⁶⁴ S. Petrak,⁶⁴ H. Quinn,⁶⁴ B. N. Ratcliff,⁶⁴ S. H. Robertson,⁶⁴ L. S. Rochester,⁶⁴ A. Roodman,⁶⁴ T. Schietinger,⁶⁴ R. H. Schindler,⁶⁴ J. Schwiening,⁶⁴ J. T. Seeman,⁶⁴ V. V. Serbo,⁶⁴ A. Snyder,⁶⁴ A. Soha,⁶⁴ S. M. Spanier,⁶⁴ J. Stelzer,⁶⁴ D. Su,⁶⁴ M. K. Sullivan,⁶⁴ H. A. Tanaka,⁶⁴ J. Va'vra,⁶⁴ S. R. Wagner,⁶⁴ A. J. R. Weinstein,⁶⁴ U. Wienands,⁶⁴ W. J. Wisniewski,⁶⁴ D. H. Wright,⁶⁴ C. C. Young,⁶⁴ P. R. Burchat,⁶⁵ C. H. Cheng,⁶⁵ D. Kirkby,⁶⁵ T. I. Meyer,⁶⁵ C. Roat,⁶⁵ A. De Silva,⁶⁶ R. Henderson,⁶⁶ W. Bugg,⁶⁷ H. Cohn,⁶⁷ A. W. Weidemann,⁶⁷ J. M. Izen,⁶⁸ I. Kitayama,⁶⁸ X. C. Lou,⁶⁸ M. Turcotte,⁶⁸ F. Bianchi,⁶⁹ M. Bona,⁶⁹ B. Di Girolamo,⁶⁹ D. Gamba,⁶⁹ A. Smol,⁶⁹ D. Zanin,⁶⁹ L. Bosisio,⁷⁰ G. Della Ricca,⁷⁰ L. Lanceri,⁷⁰ A. Pompili,⁷⁰ P. Poropat,⁷⁰ G. Vuagnin,⁷⁰ R. S. Panvini,⁷¹ C. M. Brown,⁷² R. Kowalewski,⁷² J. M. Roney,⁷² H. R. Band,⁷³ E. Charles,⁷³ S. Dasu,⁷³ F. Di Lodovico,⁷³ A. M. Eichenbaum,⁷³ H. Hu,⁷³ J. R. Johnson,⁷³ R. Liu,⁷³ J. Nielsen,⁷³ Y. Pan,⁷³ R. Prepost,⁷³ I. J. Scott,⁷³ S. J. Sekula,⁷³ J. H. von Wimmersperg-Toeller,⁷³ S. L. Wu,⁷³ Z. Yu,⁷³ H. Zobernig,⁷³ T. M. B. Kordich,⁷⁴ and H. Neal⁷⁴

(BABAR Collaboration)

¹Laboratoire de Physique des Particules, F-74941 Annecy-le-Vieux, France

²Università di Bari, Dipartimento di Fisica and INFN, I-70126 Bari, Italy

³Institute of High Energy Physics, Beijing 100039, China

⁴University of Bergen, Institute of Physics, N-5007 Bergen, Norway

⁵Lawrence Berkeley National Laboratory and University of California, Berkeley, California 94720

⁶University of Birmingham, Birmingham B15 2TT, United Kingdom

⁷Ruhr Universität Bochum, Institut für Experimentalphysik 1, D-44780 Bochum, Germany

⁸University of Bristol, Bristol BS8 1TL, United Kingdom

⁹University of British Columbia, Vancouver, British Columbia, Canada V6T 1Z1

¹⁰Brunel University, Uxbridge, Middlesex UB8 3PH, United Kingdom

¹¹Budker Institute of Nuclear Physics, Novosibirsk 630090, Russia

¹²University of California at Irvine, Irvine, California 92697

¹³University of California at Los Angeles, Los Angeles, California 90024

¹⁴University of California at San Diego, La Jolla, California 92093

¹⁵University of California at Santa Barbara, Santa Barbara, California 93106

¹⁶University of California at Santa Cruz, Institute for Particle Physics, Santa Cruz, California 95064

¹⁷California Institute of Technology, Pasadena, California 91125

¹⁸University of Cincinnati, Cincinnati, Ohio 45221

¹⁹University of Colorado, Boulder, Colorado 80309

²⁰Colorado State University, Fort Collins, Colorado 80523

²¹Technische Universität Dresden, Institut für Kern- und Teilchenphysik, D-01062 Dresden, Germany

²²Ecole Polytechnique, F-91128 Palaiseau, France

- ²³University of Edinburgh, Edinburgh EH9 3JZ, United Kingdom
²⁴Elon University, Elon University, North Carolina 27244-2010
²⁵Università di Ferrara, Dipartimento di Fisica and INFN, I-44100 Ferrara, Italy
²⁶Florida A&M University, Tallahassee, Florida 32307
²⁷Laboratori Nazionali di Frascati dell'INFN, I-00044 Frascati, Italy
²⁸Università di Genova, Dipartimento di Fisica and INFN, I-16146 Genova, Italy
²⁹Harvard University, Cambridge, Massachusetts 02138
³⁰University of Iowa, Iowa City, Iowa 52242
³¹Iowa State University, Ames, Iowa 50011-3160
³²Laboratoire de l'Accélérateur Linéaire, F-91898 Orsay, France
³³Lawrence Livermore National Laboratory, Livermore, California 94550
³⁴University of Liverpool, Liverpool L69 3BX, United Kingdom
³⁵University of London, Imperial College, London SW7 2BW, United Kingdom
³⁶Queen Mary, University of London, E1 4NS, United Kingdom
³⁷University of London, Royal Holloway and Bedford New College, Egham, Surrey TW20 0EX, United Kingdom
³⁸University of Louisville, Louisville, Kentucky 40292
³⁹University of Manchester, Manchester M13 9PL, United Kingdom
⁴⁰University of Maryland, College Park, Maryland 20742
⁴¹University of Massachusetts, Amherst, Massachusetts 01003
⁴²Massachusetts Institute of Technology, Laboratory for Nuclear Science, Cambridge, Massachusetts 02139
⁴³McGill University, Montréal, Québec, Canada H3A 2T8
⁴⁴Università di Milano, Dipartimento di Fisica and INFN, I-20133 Milano, Italy
⁴⁵University of Mississippi, University, Mississippi 38677
⁴⁶Université de Montréal, Laboratoire René J.A. Lévêque, Montréal, Québec, Canada H3C 3J7
⁴⁷Mount Holyoke College, South Hadley, Massachusetts 01075
⁴⁸Università di Napoli Federico II, Dipartimento di Scienze Fisiche and INFN, I-80126 Napoli, Italy
⁴⁹University of Notre Dame, Notre Dame, Indiana 46556
⁵⁰Oak Ridge National Laboratory, Oak Ridge, Tennessee 37831
⁵¹University of Oregon, Eugene, Oregon 97403
⁵²Università di Padova, Dipartimento di Fisica and INFN, I-35131 Padova, Italy
⁵³Universités Paris VI et VII, Lab de Physique Nucléaire H. E., F-75252 Paris, France
⁵⁴Università di Pavia, Dipartimento di Elettronica and INFN, I-27100 Pavia, Italy
⁵⁵University of Pennsylvania, Philadelphia, Pennsylvania 19104
⁵⁶Università di Pisa, Scuola Normale Superiore and INFN, I-56010 Pisa, Italy
⁵⁷Prairie View A&M University, Prairie View, Texas 77446
⁵⁸Princeton University, Princeton, New Jersey 08544
⁵⁹Università di Roma La Sapienza, Dipartimento di Fisica and INFN, I-00185 Roma, Italy
⁶⁰Universität Rostock, D-18051 Rostock, Germany
⁶¹Rutherford Appleton Laboratory, Chilton, Didcot, Oxon, OX11 0QX, United Kingdom
⁶²DAPNIA, Commissariat à l'Energie Atomique/Saclay, F-91191 Gif-sur-Yvette, France
⁶³University of South Carolina, Columbia, South Carolina 29208
⁶⁴Stanford Linear Accelerator Center, Stanford, California 94309
⁶⁵Stanford University, Stanford, California 94305-4060
⁶⁶TRIUMF, Vancouver, British Columbia, Canada V6T 2A3
⁶⁷University of Tennessee, Knoxville, Tennessee 37996
⁶⁸University of Texas at Dallas, Richardson, Texas 75083
⁶⁹Università di Torino, Dipartimento di Fisica Sperimentale and INFN, I-10125 Torino, Italy
⁷⁰Università di Trieste, Dipartimento di Fisica and INFN, I-34127 Trieste, Italy
⁷¹Vanderbilt University, Nashville, Tennessee 37235
⁷²University of Victoria, Victoria, British Columbia, Canada V8W 3P6
University of Wisconsin, Madison, Wisconsin 53706
⁷⁴Yale University, New Haven, Connecticut 06511

(Received 25 October 2001; published 26 February 2002)

The branching fractions of the exclusive decays $B^0 \rightarrow K^{*0} \gamma$ and $B^+ \rightarrow K^{*+} \gamma$ are measured from a sample of $(22.74 \pm 0.36) \times 10^6$ $B\bar{B}$ decays collected with the BABAR detector at the PEP-II asymmetric e^+e^- collider. We find $\mathcal{B}(B^0 \rightarrow K^{*0} \gamma) = [4.23 \pm 0.40(\text{stat}) \pm 0.22(\text{syst})] \times 10^{-5}$, $\mathcal{B}(B^+ \rightarrow K^{*+} \gamma) = [3.83 \pm 0.62(\text{stat}) \pm 0.22(\text{syst})] \times 10^{-5}$ and constrain the CP -violating charge asymmetry to be $-0.170 < A_{CP}(B \rightarrow K^* \gamma) < 0.082$ at 90% C.L.

In the standard model (SM) the exclusive decays $B \rightarrow K^* \gamma$ proceed dominantly by the electromagnetic loop “penguin” transition $b \rightarrow s \gamma$. Many extensions of the SM provide new virtual high-mass fermions and bosons that can appear in the loop, causing deviations in the inclusive rate for $b \rightarrow s \gamma$ [1]. The sensitivity of the exclusive rates to these effects is limited by the uncertainty in the SM calculation. However, there has been considerable theoretical progress recently [2]. The precision measurement of the exclusive branching fractions $\mathcal{B}(B^0 \rightarrow K^{*0} \gamma)$, $\mathcal{B}(B^+ \rightarrow K^{*+} \gamma)$ is needed to test and improve these calculations. The non-SM processes can also interfere with the SM decay to cause CP -violating charge asymmetries at a level as high as 20% [3]. The CP -violating charge asymmetry from SM contributions alone is expected to be $< 1\%$.

In this Letter, measurements of the exclusive branching fractions, $\mathcal{B}(B^0 \rightarrow K^{*0} \gamma)$ in the $K^{*0} \rightarrow K^+ \pi^-$, $K_S^0 \pi^0$ modes, and $\mathcal{B}(B^+ \rightarrow K^{*+} \gamma)$ in the $K^{*+} \rightarrow K^+ \pi^0$, $K_S^0 \pi^+$ modes with $K_S^0 \rightarrow \pi^+ \pi^-$, are presented. Here K^* refers to the $K^*(892)$ resonance and the charge conjugate decays are implied unless otherwise stated. The $K^{*0} \rightarrow K^+ \pi^-$ and $K^{*+} \rightarrow K^+ \pi^0$, $K_S^0 \pi^+$ modes are used to search for CP -violating charge asymmetries.

The data were collected with the *BABAR* detector [4] at the PEP-II asymmetric $e^+(3.1 \text{ GeV}) - e^-(9 \text{ GeV})$ storage ring [5]. The results in this paper are based upon an integrated luminosity of $\approx 20.7 \text{ fb}^{-1}$ of data corresponding to $(22.74 \pm 0.36) \times 10^6$ $B\bar{B}$ meson pairs recorded at the $\Upsilon(4S)$ resonance (“on-resonance”) and $\approx 2.6 \text{ fb}^{-1}$ at 40 MeV below this energy (“off-resonance”). The number of $B\bar{B}$ meson pairs is determined from the ratio of the number of hadronic events to muon pairs in on- and off-resonance data [4]. We assume that the $\Upsilon(4S)$ decays equally to neutral and charged B meson pairs.

We use Monte Carlo simulations of the *BABAR* detector based on GEANT 3.21 [6] to optimize our selection criteria and to determine signal efficiencies. Events taken from random triggers are used to measure the beam backgrounds. These simulations take account of varying detector conditions and beam backgrounds.

The selection criteria for this analysis are optimized to maximize $S^2/(S+B)$ where S is the number of signal candidates expected, assuming the central values of the previous measurement $\mathcal{B}(B^0 \rightarrow K^{*0} \gamma, B^+ \rightarrow K^{*+} \gamma) = [4.55_{-0.68}^{+0.72}(\text{stat}) \pm 0.34(\text{syst}), 3.76_{-0.83}^{+0.89}(\text{stat}) \pm 0.28(\text{syst})] \times 10^{-5}$ [7], and B is the expected number of background candidates determined from Monte Carlo and confirmed with off-resonance data. Quantities are computed in both the laboratory frame and the center-of-mass frame of the e^+e^- system. Those computed in the center-of-mass frame are denoted by an asterisk; e.g., $E_{\text{beam}}^* = 5.29 \text{ GeV}$ is the on-resonance center-of-mass energy of the e^+ and e^- beams.

We require a high-energy radiative photon candidate with energy $1.5 < E_\gamma < 4.5 \text{ GeV}$ in the laboratory frame and $2.30 < E_\gamma^* < 2.85 \text{ GeV}$ in the center-of-mass frame.

A photon candidate is defined as a localized energy maximum [4] in the calorimeter acceptance $-0.74 < \cos\theta < 0.93$, where θ is the polar angle to the detector axis. It must be isolated by 25 cm from any other photon candidate or track and have a lateral energy profile consistent with a photon shower. We veto photons from a $\pi^0(\eta)$ by requiring that the invariant mass of the combination with any other photon of energy greater than 50(250) MeV not be within a $\approx 2.7(2.2)$ sigma window of the nominal $\pi^0(\eta)$ mass, $115(508) < M_{\gamma\gamma} < 155(588) \text{ MeV}/c^2$.

The K^* is reconstructed from K^+ , K_S^0 , π^- , and π^0 candidates through the four modes $K^{*0} \rightarrow K^+ \pi^-$, $K_S^0 \pi^0$ and $K^{*+} \rightarrow K^+ \pi^0$, $K_S^0 \pi^+$. The K^+ and π^- track candidates are required to be well reconstructed in the drift chamber and to originate from a vertex consistent with the e^+e^- interaction point (IP). The K_S^0 candidates are reconstructed from two oppositely charged tracks coming from a common vertex displaced from the IP by at least 0.2 cm and having an invariant mass within ≈ 3.3 sigma of the nominal K_S^0 mass, $489 < M_{\pi^+\pi^-} < 507 \text{ MeV}/c^2$. A track is identified as a kaon if it is projected to pass through the fiducial volume of the particle identification detector, an internally reflecting ring-imaging Cherenkov detector (DIRC) [4], and the cone of Cherenkov light is consistent in time and angle with a kaon of the measured track momentum. A charged pion is identified as a track that is not a kaon. The π^0 candidates are reconstructed from pairs of photons, each with energy greater than 30 MeV, and are required to have $115 < M_{\gamma\gamma} < 150 \text{ MeV}/c^2$ and $E_{\pi^0} > 200 \text{ MeV}$. A mass-constraint fit to the nominal π^0 mass is used to improve the resolution of its momentum. The K^* reconstruction is completed by requiring the invariant mass of the candidate pairs to be within $100 \text{ MeV}/c^2$ of the K^{*0}/K^{*+} mass.

The B meson candidates are reconstructed from the K^* and γ candidates. The background is predominantly from continuum $q\bar{q}$ production, where q can be a u , d , s , or c quark, with the high-energy photon originating from initial-state radiation or from π^0 and η decays. The background from other nonradiative B meson decays is found to be negligible from Monte Carlo simulation. We exploit event topology differences between signal and background to reduce the continuum contribution. We compute the thrust axis of the event excluding the B meson daughter candidates. Figure 1 shows the distribution of $|\cos\theta_T^*|$ for signal Monte Carlo events and off-resonance data, where θ_T^* is the angle between the high-energy photon candidate and the thrust axis. In the center-of-mass frame, $B\bar{B}$ pairs are produced approximately at rest and produce a uniform $|\cos\theta_T^*|$ distribution. In contrast, $q\bar{q}$ pairs are produced back-to-back in the center-of-mass frame which results in a $|\cos\theta_T^*|$ distribution peaking at 1. We require $|\cos\theta_T^*| < 0.8$. We further suppress backgrounds using the angle of the B meson candidate’s direction with respect to the beam axis, θ_B^* , and the helicity angle of the K^* decay, θ_H . The helicity angle is defined as the angle between either one of the K^* daughters’ momentum

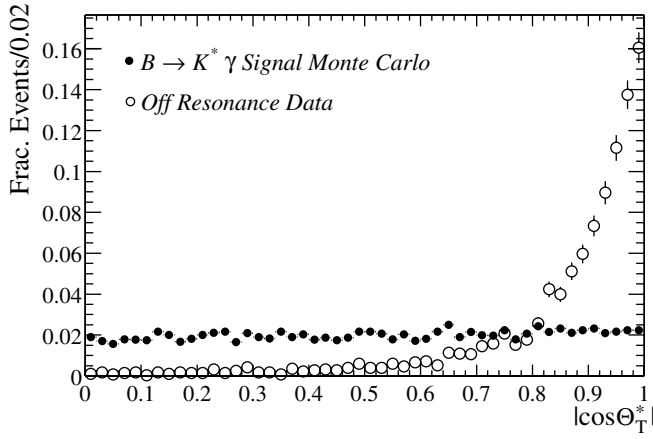


FIG. 1. The event shape variable $|\cos\theta_T^*|$ for $B^0 \rightarrow K^{*0}\gamma$, $K^{*0} \rightarrow K^+\pi^-$ Monte Carlo and off-resonance data.

vectors computed in the rest frame of the K^* and the K^* momentum vector in the parent B meson rest frame. It follows a $\sin^2\theta_H$ distribution for the signal and peaks slightly towards ± 1 for $q\bar{q}$ background. The B meson candidate's direction also follows a $\sin^2\theta_B^*$ for the signal and is approximately flat for the $q\bar{q}$ background. We require $|\cos\theta_B^*| < 0.80$ and $|\cos\theta_H| < 0.75$.

Since the B mesons are produced via $e^+e^- \rightarrow Y(4S) \rightarrow B\bar{B}$, the energy of the B meson in the center-of-mass frame is the beam energy, E_{beam}^* . This is compared to the measured energy of the B meson daughters by defining $\Delta E^* = E_{K^*}^* + E_\gamma^* - E_{\text{beam}}^*$. The distribution of ΔE^* is peaked at zero for the signal with a width dominated by the resolution of the photon candidates. It is asymmetric due to energy leakage from the calorimeter. We require $-200 < \Delta E^* < 100$ MeV for the $K^+\pi^-$, $K_S^0\pi^+$ modes and $-225 < \Delta E^* < 125$ MeV for the modes containing a π^0 , namely $K^+\pi^0$ and $K_S^0\pi^0$. The beam-energy substituted mass is defined as $m_{\text{ES}} = \sqrt{E_{\text{beam}}^{*2} - \mathbf{p}_B^{*2}}$, where \mathbf{p}_B^* is the momentum vector of the B meson candidate calculated from the measured momenta of the daughters. The m_{ES} distribution for the signal is well described by an asymmetric resolution function [8], with an approximately Gaussian core dominated by the resolution of the beam energy measurement, and an asymmetric tail caused by the energy leakage from the calorimeter for the photon candidates. For the modes containing a single photon candidate, namely $K^+\pi^-$ and $K_S^0\pi^+$, we can remove the tail in m_{ES} by rescaling the measured photon energy E_γ^* by a factor κ , determined for each event, so that $E_{K^*}^* + \kappa E_\gamma^* - E_{\text{beam}}^* = 0$. The signal for these modes is then described by a Gaussian. The background is empirically described by a threshold function [9] for each mode. We select candidates with $m_{\text{ES}} > 5.2$ GeV/c^2 .

Figure 2 shows the m_{ES} distribution for each of the four modes. An unbinned maximum-likelihood technique is used to fit the m_{ES} distributions for signal [8] and background [9] contributions. The signal mean and width are allowed to vary in the fit for the high statistics $K^+\pi^-$

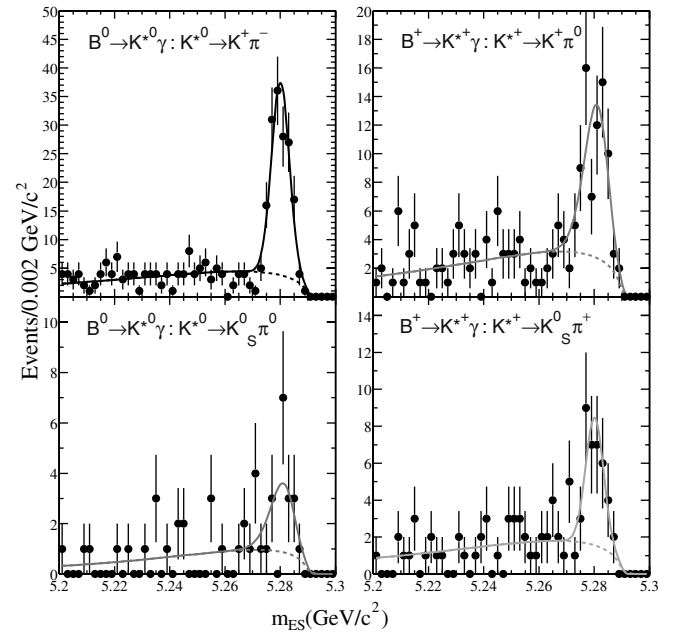


FIG. 2. m_{ES} for the $B \rightarrow K^*\gamma$ candidates. The solid and dashed curves show, respectively, the fitted signal-plus-background and the background alone. The fits used to extract the signal yield are described in the text.

and $K^+\pi^0$ modes. The fitted width is slightly larger than the predicted Monte Carlo value. In the lower statistics modes we fix the width to the Monte Carlo value adjusted for the small difference observed in the high statistics modes. We fit the on-resonance data with a signal plus background shape, and simultaneously the on-resonance sideband and off-resonance samples with the same background function, using a common fit parameter. The off-resonance data sample is required to pass the same selection criteria as the on-resonance data sample except that we remove the kaon particle identification requirement to gain statistics in the $K^+\pi^-$ and $K^+\pi^0$ modes. The on-resonance sideband sample is selected with the same criteria as the on-resonance data sample, except that we require $150 < \Delta E^* < 400$ MeV in the $K_S^0\pi^0$ and $K^+\pi^0$ modes, and $100 < \Delta E^* < 500$ MeV in the $K^+\pi^-$ and $K_S^0\pi^+$ modes. The signal yields with statistical errors from the fit are given in Table I.

As a consistency check we plot in Fig. 3a the ΔE^* projection for the $K^+\pi^-$ mode after requiring $5.27 < m_{\text{ES}} < 5.29$ GeV/c^2 . A comparison of the observed ΔE^* distribution with Monte Carlo shows good agreement. We also plot $M_{K^+\pi^-}$ in Fig. 3b after requiring $5.27 < m_{\text{ES}} < 5.29$ GeV/c^2 , $-200 < \Delta E^* < 100$ MeV, and $0.7 < M_{K^+\pi^-} < 1.1$ GeV/c^2 . We fit with a relativistic Breit-Wigner plus linear background shape and determine that the signal is consistent with coming from the $K^*(892)$.

The efficiency for the selection of $B \rightarrow K^*\gamma$ candidates is given in Table I. The branching fraction is determined from the yield, the efficiency and the total number of $B\bar{B}$ events in the sample. The cross-feed from the other $B \rightarrow K^*\gamma$ modes and the down-feed from $B \rightarrow X_S\gamma$

TABLE I. The fitted signal yield, efficiency [including $\mathcal{B}(K^*)$ and $\mathcal{B}(K^0)$], cross-feed and down-feed from other penguin decays, and measured branching fraction $\mathcal{B}(B \rightarrow K^* \gamma)$ for each of the decay modes.

Mode	Efficiency %	No. signal events	No. cross-feed events	No. down-feed events	$\mathcal{B}(B \rightarrow K^* \gamma)$ $\pm \text{stat} \pm \text{syst} \times 10^{-5}$
$K^+ \pi^-$	14.0	135.7 ± 13.3	0.4 ± 0.1	0.6 ± 0.1	$4.24 \pm 0.41 \pm 0.22$
$K_S^0 \pi^0$	1.4	14.8 ± 5.6	0.4 ± 0.1	1.0 ± 0.2	$4.10 \pm 1.71 \pm 0.42$
$K_S^0 \pi^+$	3.9	28.1 ± 6.6	0.7 ± 0.2	1.2 ± 0.2	$3.01 \pm 0.76 \pm 0.21$
$K^+ \pi^0$	4.3	57.6 ± 10.4	1.2 ± 0.2	2.6 ± 0.4	$5.52 \pm 1.07 \pm 0.38$

are estimated with Monte Carlo assuming the measured branching fractions from the CLEO Collaboration [7,10] for each mode and subtracted from the signal yield.

The total systematic error is the sum in quadrature of the components shown in Table II. The systematic uncertainty in the signal yield derives from uncertainties in the signal line shape, and cross-feed and down-feed contributions. The uncertainty in the signal line shape results from the m_{ES} width difference described above. To gain statistics in the off-resonance data sample used to fit the background function for the $K^+ \pi^-$ and $K^+ \pi^0$ modes we relax the kaon identification requirement and consequently assign a systematic uncertainty to the assumption that the background shape is unaffected. The error in the assumed branching fractions and final-state modeling for $B \rightarrow X_s \gamma$ [10] gives a systematic error in the estimated down-feed from these modes. The tracking efficiency is computed by identifying tracks in the silicon vertex detector and observing the fraction that is well reconstructed in the drift chamber. We estimate the K_S^0 efficiency uncertainty by comparing the momenta and flight-distance distributions in data and Monte Carlo. The kaon identification efficiency in the DIRC is derived from a sample of $D^{*+} \rightarrow D^0 \pi^+$, $D^0 \rightarrow K^- \pi^+$ decays. The photon and π^0 efficiencies are measured by comparing the ratio of events $N(\tau^\pm \rightarrow h^\pm \pi^0)/N(\tau^\pm \rightarrow h^\pm \pi^0 \pi^0)$ to the previously measured branching ratios [11]. The photon isolation and π^0/η veto efficiency are dependent on the event multiplicity and are tested by “embedding” Monte Carlo-generated photons into both an exclusively reconstructed

B meson data sample and a generic B meson Monte Carlo sample. The ΔE^* resolution is dominated by the photon-energy resolution so that uncertainties in the calorimeter energy resolution and overall energy-scale cause an uncertainty in the efficiency of the ΔE^* requirement. The photon-energy resolution is measured in data using π^0 and η meson decays and $e^+ e^- \rightarrow e^+ e^- \gamma$ events. The energy scale uncertainty is estimated by using a sample of η meson decays with symmetric energy photons; the deviation in the reconstructed η mass from the nominal η mass provides an estimate of the uncertainty in the measured single photon energy.

The $B \rightarrow K^* \gamma$ samples, except for the $K_S^0 \pi^0$ sample, are used to search for CP -violating charge asymmetries A_{CP} , defined by

$$A_{CP} = \frac{\Gamma(\bar{B} \rightarrow \bar{K}^* \gamma) - \Gamma(B \rightarrow K^* \gamma)}{\Gamma(\bar{B} \rightarrow \bar{K}^* \gamma) + \Gamma(B \rightarrow K^* \gamma)}.$$

The flavor of the underlying b quark is tagged by the charge of the K^\pm or $K^{*\pm}$ in the decay. The probability of a double misidentification of the kaon and pion, which would result in a dilution of the asymmetry, is estimated to be 0.0026 ± 0.0008 and has been neglected. The on-resonance sample for each mode is divided into two CP -conjugate samples and the signal yield for each is extracted with the same fitting technique as for the branching

TABLE II. The systematic uncertainties in the measurement of $\mathcal{B}(B \rightarrow K^* \gamma)$.

	% Uncertainty in $\mathcal{B}(B \rightarrow K^* \gamma)$			
	$K^+ \pi^-$	$K_S^0 \pi^0$	$K_S^0 \pi^+$	$K^+ \pi^0$
m_{ES} line shape	...	7.4	1.7	1.9
Background shape	1.0	3.8
Down-feed modeling	1.0	1.5	1.0	1.2
Photon efficiency	1.3	1.3	1.3	1.3
Photon distance cut	2.0	2.0	2.0	2.0
π^0 efficiency	...	2.5	...	2.5
π^0/η veto	1.0	1.0	1.0	1.0
Energy resolution	2.5	2.5	2.5	2.5
Energy scale	1.0	1.0	1.0	1.0
K^\pm/π^\pm tracking efficiency	2.4	...	1.2	1.3
K_S^0 efficiency	...	4.5	4.5	...
Kaon identification	0.7	1.0
MC statistics	1.9	2.4	1.5	2.1
B counting	1.6	1.6	1.6	1.6
Total	5.3	10.3	6.7	7.0

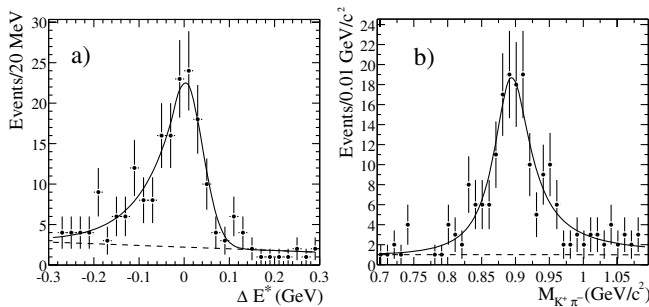


FIG. 3. (a) The ΔE^* projection for $B^0 \rightarrow K^{*0} \gamma$, $K^{*0} \rightarrow K^+ \pi^-$ candidates. The curve is the Monte Carlo expectation with a linear background. (b) The $M_{K^+ \pi^-}$ projection for $B^0 \rightarrow K^{*0} \gamma$, $K^{*0} \rightarrow K^+ \pi^-$ candidates with the $M_{K^+ \pi^-}$ mass cut relaxed. The curve is a fit to a relativistic Breit-Wigner function with linear background.

TABLE III. The measured A_{CP} in signal and background samples.

Mode	A_{CP} (signal) (\pm stat \pm syst)	A_{CP} (background) (\pm stat)
$K^+ \pi^-$	$-0.049 \pm 0.094 \pm 0.012$	-0.011 ± 0.104
$K_S^0 \pi^+$	$-0.190 \pm 0.210 \pm 0.012$	-0.080 ± 0.080
$K^+ \pi^0$	$0.044 \pm 0.155 \pm 0.021$	-0.022 ± 0.105

fraction measurements. In the fit the background shape and normalization, as well as the signal peak and width, are constrained to be the same for both CP -conjugate samples. The measured asymmetries and the asymmetry of the background in the sideband regions defined by $-200 < \Delta E^* < 100$ MeV, $5.2 < m_{ES} < 5.27$ GeV/ c^2 are given in Table III.

The systematic uncertainty in the asymmetry is due to possible detector effects that cause a different reconstruction efficiency for the two CP conjugate decays. This uncertainty has been estimated with data from a number of known charge-symmetric processes and is given in Table III.

Finally, we combine the measured branching fractions for the individual modes using a weighted average, $\mathcal{B}(B^+ \rightarrow K^{*+} \gamma) = [3.83 \pm 0.62(\text{stat}) \pm 0.22(\text{syst})] \times 10^{-5}$, $\mathcal{B}(B^0 \rightarrow K^{*0} \gamma) = [4.23 \pm 0.40(\text{stat}) \pm 0.22(\text{syst})] \times 10^{-5}$. The weighting uses the quadratic sum of the statistical and uncorrelated systematic errors, and the combined error takes into account the correlated systematic errors. The weighted average of the measured CP -violating charge asymmetries is $A_{CP}(B \rightarrow K^* \gamma) = -0.044 \pm 0.076(\text{stat}) \pm 0.012(\text{syst})$. We constrain $-0.170 < A_{CP}(B \rightarrow K^* \gamma) < 0.082$ at 90% C.L.

We are grateful for the excellent luminosity and machine conditions provided by our PEP-II colleagues. The collaborating institutions wish to thank SLAC for its support and kind hospitality. This work is supported by DOE and NSF, NSERC (Canada), IHEP (China), CEA and

CNRS-IN2P3 (France), BMBF (Germany), INFN (Italy), NFR (Norway), MIST (Russia), and PPARC (United Kingdom). Individuals have received support from the Swiss NSF, A. P. Sloan Foundation, Research Corporation, and Alexander von Humboldt Foundation.

*Also with Università di Perugia, Perugia, Italy.

†Also with Università della Basilicata, Potenza, Italy.

- [1] See, for example, S. Bertolini, F. Borzumati, and A. Masiero, Phys. Lett. B **192**, 437 (1987); H. Baer and M. Brhlik, Phys. Rev. D **55**, 3201 (1997); J. Hewett and J. Wells, Phys. Rev. D **55**, 5549 (1997); M. Carena *et al.*, Phys. Lett. B **499**, 141 (2001).
- [2] M. Beneke, T. Feldmann, and D. Seidel, hep-ph/0106067; S. W. Bosch and G. Buchalla, hep-ph/0106081; A. Kagan and M. Neubert, hep-ph/0110078; Z. Ligeti and M. B. Wise, Phys. Rev. D **60**, 117506 (1999).
- [3] A. Kagan and M. Neubert, Phys. Rev. D **58**, 094012 (1998).
- [4] *BABAR* Collaboration, B. Aubert *et al.*, hep-ex/0105044 [Nucl. Instrum. Methods (to be published)].
- [5] PEP-II Conceptual Design Report, SLAC-0418, 1993.
- [6] "GEANT Detector Description and Simulation Tool," CERN Program Library Long Writeup W5013, 1994.
- [7] CLEO Collaboration, T. Coan *et al.*, Phys. Rev. Lett. **84**, 5283 (2000).
- [8] The signal for the $K^+ \pi^0$ and $K_S^0 \pi^0$ modes is fit with the function $dN/dm_{ES} = A_S \exp(-0.5\{\ln^2[1 + \Lambda\tau(m_{ES} - m_0)]/\tau^2 + \tau^2\})$ where $\Lambda = \sinh(\tau\sqrt{\ln 4})/(\sigma\tau\sqrt{\ln 4})$, the peak position is m_0 , the width is σ , and τ is the tail parameter. The $K^+ \pi^-$ and $K_S^0 \pi^+$ modes are fit with a Gaussian distribution.
- [9] The background for each mode is fit with $dN/dm_{ES} = A_B m_{ES} \sqrt{1 - m_{ES}^2/E_{\text{beam}}^{*2}} \exp[-\zeta(1 - m_{ES}^2/E_{\text{beam}}^{*2})]$, a function introduced by the ARGUS Collaboration, H. Albrecht *et al.*, Z. Phys. C **48**, 543 (1990).
- [10] CLEO Collaboration, S. Chen *et al.*, hep-ex/0108032.
- [11] CLEO Collaboration, M. Procaro *et al.*, Phys. Rev. Lett. **70**, 1207 (1993).